

Variable Effects of Climate on Forest Growth in Relation to Ecosystem State

Malcolm S. Itter ¹

*Department of Forestry, Michigan State University, East Lansing, Michigan 48824 USA
Program in Ecology, Evolutionary Biology, and Behavior, Michigan State University, East Lansing,
Michigan 48824 USA*

Andrew O. Finley ²

*Department of Forestry, Michigan State University, East Lansing, Michigan 48824 USA
Department of Geography, Michigan State University, East Lansing, Michigan 48824 USA*

Anthony W. D'Amato ³

*Rubenstein School of the Environment and Natural Resources, University of Vermont, Burlington, Vermont
05405 USA*

Jane R. Foster ⁴

Department of Forest Resources, University of Minnesota, St. Paul, Minnesota 55108 USA

John B. Bradford ⁵

Southwest Biological Science Center, U.S. Geological Survey, Flagstaff, Arizona 86001 USA

¹ittermal@msu.edu

²finleya@msu.edu

³awdamato@uvm.edu

⁴jrfoster@umn.edu

⁵jbradford@usgs.gov

1 Abstract

Tree growth rings are regularly applied in forest ecology to understand the relationship between climate and forest growth. To this end, individual trees considered sensitive to climate are sampled and the average effects of climate over the sample period are estimated. Forests are dynamic systems, the structure, composition, and health of which evolve over time. The relationship between climate and forest growth is likely to change in relation to fundamental shifts in a forest ecosystem. Identifying and understanding changes in the growth-climate relationship requires data from entire forest systems and models that estimate the effects of climate on forest growth as a function of ecosystem state. We develop a Bayesian hierarchical model that: 1) allows the effects of climate to vary temporally using a state space framework; 2) allows for error propagation across tree growth ring standardization steps; and, 3) applies climate data at an appropriate spatial scale. The model is applied to tree ring census data from forests in northeastern Minnesota. Important climate variables are identified using Bayesian variable selection. Results indicate forest growth is most sensitive to the interactive effects of temperature and precipitation represented through water balance metrics. We observe changes in forest growth response to water balance variables over time with distinct periods of increased sensitivity to water availability. Periods of increased sensitivity correspond to droughts and forest tent caterpillar outbreak years in which the structure and function of study forests change. Variation in the response of tree growth due to climatic extremes or disturbance events are not observable applying conventional dendrochronology models that estimate the average effects of climate on tree growth over time. Our results are one example of additional inferences made possible by using a Bayesian state space approach to model tree growth as a function of climate. Extensions to the model can be used to analyze the interaction between climate and forest ecosystem dynamics. The state space approach is not limited to tree growth analyses, but can be applied in any ecological analysis focused on understanding the effects of climate on ecosystem processes.

Keywords

Bayesian state space model, climate, disturbance, forest dynamics, forest tent caterpillar, hierarchical models, productivity/biomass, tree rings

2 Introduction

There is a well established correlation between annual tree growth increments (hereafter “growth rings”) and climate variability. Dendrochronologists have long leveraged this correlation to infer historic climates from growth rings (Fritts 1976). While understanding past climates is important, a major focus of contemporary forest ecology is understanding the relationship between climate and forest processes. In particular, forest ecologists seek to understand the mechanisms by which climate affects forest productivity—the growth-climate relationship (Littell et al. 2008; Carrer 2011; Leites et al. 2012; Dymond et al. 2015). Forest productivity is directly related to terrestrial carbon pools and atmosphere-biosphere interactions such that changes in forest productivity may impact the global carbon cycle leading to feedbacks that alter the rate of global climate change (Bonan 2008). Understanding the mechanisms underlying the growth-climate relationship

enables prediction of changes to forest growth under novel future climates and their potential effects on the global carbon cycle. Growth rings are useful data in this regard given their functional connection to radial tree growth, basal area, and above-ground biomass, and their correlation with climate (Babst et al. 2014).

Forests are dynamic systems. The size (e.g. basal area, biomass), structure, and fundamental processes of tree establishment, growth, mortality, and decomposition that define a forest ecosystem change over time and space in relation to ecological factors including successional stage, species assemblage, disturbance, and forest health. Throughout, we refer to the size, structure, and processes that define a forest ecosystem as the *forest ecosystem state*. Given the dynamic nature of forest ecosystems, it is reasonable to hypothesize that the effects of climate on tree growth change dependent on forest ecosystem state and as a result vary over time and space. Understanding how the growth-climate relationship changes as a function of ecosystem state is an important step toward learning the mechanisms driving the effects of climate on forest productivity. From a management perspective, the ability to predict changes in forest growth response to climate due to shifts in the forest system is critical to the success of long-term management plans under novel climatic conditions.

Dendrochronology has an extensive literature on techniques to model tree growth as a function of climate that focus on modeling individual growth or average growth for a selection of trees considered “sensitive” to climate, that is, trees that are free of competition, exhibit no growth defects, and are of good health and above average size (Cook and Kairiukstis 1990). Growth rings are crossdated and standardized to generate a growth chronology that is compared to climate variables of interest using either a correlation analysis or regression model. Regardless of the approach applied, the effect of climate on a growth chronology (i.e. the correlation or regression coefficient) is fixed with respect to time and represents the average effect of climate on growth during the study period. While this approach is effective for reconstructing past climates, to understand the relationship between climate and forest productivity we need to consider the entire forest ecosystem and how the current state of a forest system interacts with climate to affect productivity. This requires: censused tree growth data from closed canopy forests that contain climate and ecosystem dynamics signals—competition, stress, disturbance; and, models that reimagine classical dendrochronology techniques to integrate and account for the biotic and abiotic factors that constitute a forest ecosystem, and complex interactions between these factors and climate. An alternative to the correlation and regression approaches used in dendrochronology to estimate the average effect of climate on tree growth over a period of interest is to apply a state space model that allows the effects of climate to vary over time, space, or both (Cressie and Wikle 2011). The utility of hierarchical state space models to understand and predict dynamic ecological processes has been demonstrated in studies of biodiversity (Clark et al. 2012), population dynamics (Calder et al. 2003; Clark and Bjørnstad 2004; Parslow et al. 2013), and invasive species (Wikle 2003; Hooten et al. 2007). Hierarchical state space models have also been used to assimilate growth ring and diameter tape measurements of radial tree growth (Clark et al. 2007; Schliep et al. 2014).

There are several additional improvements that can be made to dendrochronology and forest ecology models to further understanding of the growth-climate relationship. The crossdating and standardization steps used to generate a growth chronology are applied separately and independently in dendrochronology (Cook and Kairiukstis 1990). Further, the growth chronology is treated as data in subsequent climate analyses. This approach does not account for errors

introduced in the crossdating and standardization procedures that may bias inference regarding the effects of climate on tree growth. Forest ecologists are frequently interested in individual tree-level variability in growth responses to climate given this variability reflects microsite, genetic, and inter-tree competition and facilitation effects (Carrer 2011; Galván et al. 2014). Climate data are frequently defined on a coarse spatial grid (e.g. 1-5 kilometer resolution) with individual observations representing the average climate within a given grid cell. Current approaches to estimate individual-level growth response variability apply spatially coarse climate data to individual trees implicitly treating climate data as if it were observed on a continuous spatial scale and representative of the microclimatic conditions experienced by individual trees. An alternative, preferable approach to current dendrochronology and forest ecology models is to apply a hierarchical or multilevel structure that moves dendrochronology standardization steps into a single model framework allowing for statistically proper error propagation and estimates tree growth response to climate at a spatial scale consistent with climate data. There are several existing model-based approaches to dendrochronology that address some of these issues (Van Deusen 1989; Schofield et al. 2015). Van Deusen (1989) develops a state space framework to estimate temporally-varying climate effects on annual growth increments. The purpose of the state space framework is to identify shifts in tree growth response to climate attributable to changes in forest density or exogenous factors such as regional air pollution. However, the model framework does not address the issue of the appropriate spatial scale at which to apply climate data. Schofield et al. (2015) develop a model-based approach to climate reconstruction using growth rings that moves standardization steps into a Bayesian hierarchical model (BHM) allowing for proper error propagation, but do not allow climatic effects to evolve over time.

We hypothesize that the effects of climate on annual tree growth vary over time in relation to ecosystem state. We develop a Bayesian hierarchical state space model that builds on the previous work of Van Deusen (1989) and Schofield et al. (2015) to test this hypothesis. The BHM allows for: 1) the effects of climate on tree growth to vary over time; 2) proper error propagation across dendrochronology standardization steps; and, 3) inference on climate variables at a spatial scale consistent with climate data. We test our hypothesis by applying the model to growth ring records from closed canopy forests in northeastern Minnesota, analyzing the evolution of climate effects over the study period in relation to ecological factors that impact forest ecosystem state. In addition to testing our hypothesis, the goal of the analysis is to demonstrate the additional insight gained regarding the effects of climate on tree growth by allowing the growth-climate relationship to vary over time in relation to ecosystem state.

3 Modeling Approach

We apply two models to estimate tree growth as a function of climate. The first serves as our base model and moves dendrochronology standardization steps into a BHM. We refer to this model throughout as the *fixed climate effects* model. The second model extends the fixed climate effects model to estimate temporally-varying climate effects using a Bayesian state space approach. We refer to this model throughout as the *variable climate effects* model.

Fixed Climate Effects

The fixed climate effects (FCE) model mimics a dendrochronology analysis where the objective is to estimate the average effect of a set of climate variables on annual tree growth over a study period. The goal of the FCE model is to move dendrochronology standardization steps into a BHM allowing for statistically proper error propagation and to apply climate observations at an appropriate spatial scale. We begin by decomposing individual tree growth rings into component sources of variability. Specifically,

$$\begin{array}{ccccccc} \textit{Individual} & = & \textit{Long-term} & + & \textit{Inter-annual} & + & \textit{Random} \\ \textit{Tree Growth} & & \textit{Trend} & & \textit{Variability} & & \textit{Error} \end{array}$$

where the long-term trend captures low-frequency changes in growth due to tree size and age, the inter-annual variability captures high-frequency changes in growth thought to be driven by climate, and the random error term captures residual variability.

Long-Term Trend: A smoothing spline is commonly applied in dendrochronology to model the long-term, low-frequency trend in individual growth attributable to tree size and age (Cook and Peters 1981). Smoothing splines are a highly flexible method to model natural phenomena using a set of polynomial basis functions (Wood 2006). Alternatives to a smoothing spline include a negative exponential regression model or a generalized additive model (Cook 1987; Fajardo and McIntire 2012). We apply a penalized spline regression model instead of a smoothing spline as it achieves equivalent smoothing with fewer model parameters (Wood 2006). Unlike a smoothing spline in which knots are defined for every observation, in a penalized spline regression model, a set of knots less than or equal to the number of observations is specified and regression coefficients are penalized such that the coefficient values for non-informative knots are forced to zero (see Appendix A for additional detail). We apply natural cubic spline basis functions evaluated at equally spaced knots defined for tree age to estimate the long-term growth trend.

Inter-Annual Variability: High-frequency, inter-annual growth variability is frequently shared across individual trees within a forest stand, hence the use of growth chronologies in studies of tree growth and climate. We model inter-annual growth variability with an additive annual stand effect that represents the average deviation of each tree within a stand from the tree's long-term growth trend within a given year. Inter-annual variation in the additive stand effect is in turn modeled as a function of observed climate. The coarse spatial scale of climate observations is consistent with forest stand-level growth response rather than individual tree growth response (Zhu et al. 2014). The use of climate observations to estimate annual stand effects acknowledges the shared response to climate among trees within a stand and applies climate observations at an appropriate spatial scale.

Random Error: The residual error is modeled using an autoregressive process to explicitly account for temporal autocorrelation in annual tree growth increments. Specifically, we apply a first order autoregressive (AR1) model for the residual error. We note the residual error can also be modeled as a function of the mean growth increment to account for heteroscedasticity. We did not choose to do so here.

Log Transformation: We model annual tree growth increments on the log-scale to ensure positive growth estimates consistent with Clark et al. (2007). Log transforming growth increments results in multiplicative errors equivalent to modeling non-transformed growth increments using a

negative exponential model (as discussed in Schofield et al. 2015). Log transforming growth increments also reduces the heteroscedasticity frequently observed in tree growth ring records.

Model Specification: Combining the component sources of variability and log transformation, we model annual tree growth increments in a BHM as follows. Let i index individual trees ($i = 1, \dots, n$), j index stands ($j = 1, \dots, k$), and t index years ($t = 1, \dots, T$) where n , k , and T are the total number of trees, stands, and years, respectively. Let $j(i)$ indicate the stand j in which the i th tree is located (e.g. $j(i) = 3$ indicates the i th tree is located in stand 3). Finally, define y to be the observed growth increment, such that $y_{i,t}$ is the observed growth increment for tree i in year t . Individual tree growth is modeled as,

$$\log(y_{i,t}) = \mathbf{x}'_{i,t}\boldsymbol{\beta}_i + \alpha_{j(i),t} + \epsilon_{i,t} \quad (1)$$

$$\epsilon_{i,t} = \phi\epsilon_{i,t-1} + e_{i,t} \quad (2)$$

$$e_{i,t} \sim \mathcal{N}(0, \sigma_{pe}^2) \quad (3)$$

where $\mathbf{x}_{i,t}$ is a p -dimensional vector of known covariate values corresponding to a set of natural cubic spline basis functions defined for tree age at p knots, $\boldsymbol{\beta}_i$ is a p -dimensional vector of tree-specific spline regression coefficients, $\alpha_{j(i),t}$ is the additive effect of being located in stand j during year t , and $\epsilon_{i,t}$ is the residual error. The residual error is modeled as an AR1 process where ϕ is an unknown correlation coefficient and $e_{i,t}$ is a pure error term (2). We assume the pure error term follows a zero-centered normal distribution with pure error variance σ_{pe}^2 (3). The AR1 error model and normality assumption for $e_{i,t}$ induces the follow distribution for $\epsilon_{i,t}$,

$$\epsilon_{i,t} \sim \mathcal{N}\left(0, \frac{\sigma_{pe}^2}{1 - \phi^2}\right)$$

where the $\epsilon_{i,t}$'s are temporally correlated. Specifically, $\text{Cor}(\epsilon_{i,t}, \epsilon_{i,t-h}) = \phi^h$ where h is the lag, $h = 0, \dots, T_i$, given tree i is observed for a total of T_i years. We assume the growth of individual trees within and across stands is independent based on exploratory analysis assessing spatial dependence ($\epsilon_{i,t} \perp \epsilon_{i',t'} \forall i \neq i', t = 1, \dots, T_i$, and $t' = 1, \dots, T_{i'}$). Stand effects are modeled using observed climate as,

$$\alpha_{j,t} = \mathbf{f}'_{j,t}\boldsymbol{\theta} + v_{j,t}$$

$$v_{j,t} \sim \mathcal{N}(0, \tau^2)$$

where $\mathbf{f}_{j,t}$ is an l -dimensional vector of observed, standardized climate covariates, $\boldsymbol{\theta}$ is an l -dimensional vector of regression coefficients, and $v_{j,t}$ is a random error term assumed to follow a zero-centered normal distribution with inter-annual variance τ^2 . We assume stand effects are independent with respect to time both within and across stands.

We apply conjugate normal priors for the individual tree-level spline and stand-level climate regression coefficients,

$$\boldsymbol{\beta}_i \sim \mathcal{N}_p(\boldsymbol{\mu}_\beta, \sigma_\beta^2 \mathbf{S}^{-1})$$

$$\boldsymbol{\theta} \sim \mathcal{N}_l(\boldsymbol{\mu}_\theta, \sigma_\theta^2 \mathbf{I})$$

where \mathbf{S} is a $p \times p$ penalty matrix defined based on knot locations (see details in Appendix A), \mathbf{I} is an l -dimensional identity matrix, and $\boldsymbol{\mu}_\beta$, σ_β^2 , $\boldsymbol{\mu}_\theta$, and σ_θ^2 are hyperparameters. We apply uniform

priors for the AR1 correlation coefficient (ensuring the autoregressive process is stationary) and the pure error and inter-annual standard deviation parameters (Gelman 2006),

$$\begin{aligned}\phi &\sim \text{Unif}(-1, 1) \\ \sigma_{pe} &\sim \text{Unif}(a_1, b_1) \\ \tau &\sim \text{Unif}(a_2, b_2).\end{aligned}$$

The hierarchical model is fully specified after setting hyperparameter values for prior distributions ($\boldsymbol{\mu}_\beta, \sigma_\beta^2, \boldsymbol{\mu}_\theta, \sigma_\theta^2, a_1, b_1, a_2, b_2$). We discuss hyperparameter values in the Bayesian inference section.

Variable Climate Effects

The variable climate effects (VCE) model extends the FCE model to allow climate regression coefficients ($\boldsymbol{\theta}$) to vary over time. The goal of the VCE model is to analyze stand-level growth sensitivity to climate variation in relation to forest ecosystem state. The climate regression coefficients are treated as state variables in the VCE model and evolve over time such that a unique set of climate coefficients is estimated for each year in the study period ($\boldsymbol{\theta}_1, \boldsymbol{\theta}_2, \dots, \boldsymbol{\theta}_T$). The time-varying process is initialized at $\boldsymbol{\theta}_0$ with all subsequent $\boldsymbol{\theta}_t$ values informed by the set of stand effects in the same year $\boldsymbol{\alpha}_t = (\alpha_{1,t}, \dots, \alpha_{k_t,t})'$ where k_t is the number of stands with growth observations in year t . The stand effects are informed by individual tree growth observations $\mathbf{y}_t = (y_{1,t}, \dots, y_{n_t,t})'$ where n_t is the number of trees with observed growth increments in year t . The time-varying climate coefficient model structure is represented graphically in Figure 1.

[Figure 1 about here.]

The tree-level model is unchanged in the VCE model. The stand-level model is updated to integrate time-varying climate coefficients. We also add a model for the evolution of climate effects over time. We apply a first order random walk to model changes in the climate coefficients as follows,

$$\alpha_{j,t} = \mathbf{f}'_{j,t} \boldsymbol{\theta}_t + v_{j,t} \quad (4)$$

$$\boldsymbol{\theta}_t = \boldsymbol{\theta}_{t-1} + \mathbf{w}_t \quad (5)$$

$$v_{j,t} \sim \mathcal{N}(0, \tau^2)$$

$$\mathbf{w}_t \sim \mathcal{N}_l(\mathbf{0}, \boldsymbol{\Sigma}_\theta)$$

where \mathbf{w}_t is an l -dimensional process error vector following a zero-centered multivariate normal distribution with covariance matrix $\boldsymbol{\Sigma}_\theta$. Equations (4) and (5) define a state-space or dynamic linear model framework with (4) serving as the observation equation and (5) the process or state equation (West and Harrison 1997).

We apply a conjugate normal prior to initialize the climate coefficient process and a scaled inverse-Wishart prior for the process error covariance matrix (as described in Gelman et al. 2014),

$$\begin{aligned}\boldsymbol{\theta}_0 &\sim \mathcal{N}_l(\mathbf{m}_0, \mathbf{C}_0) \\ \boldsymbol{\Sigma}_\theta &= \text{Diag}(\boldsymbol{\eta})\boldsymbol{\Sigma}(\boldsymbol{\eta})\text{Diag}(\boldsymbol{\eta}) \\ \boldsymbol{\Sigma}(\boldsymbol{\eta}) &\sim \text{Inv-Wish}(\nu, \mathbf{V}) \\ \eta_s &\stackrel{\text{iid}}{\sim} \text{Unif}(a_3, b_3) \quad s = 1, \dots, l\end{aligned}$$

where $\boldsymbol{\eta}$ is an l -dimensional vector of scale parameters each assigned a uniform prior distribution, $\text{Diag}(\boldsymbol{\eta})$ indicates an l -dimensional diagonal matrix with values of $\boldsymbol{\eta}$ on the diagonal, and $\boldsymbol{\Sigma}(\boldsymbol{\eta})$ is an l -dimensional correlation matrix. All other priors remain the same as in the FCE model. Again, the model is fully specified after setting hyperparameter values for prior distributions ($\mathbf{m}_0, \mathbf{C}_0, \nu, \mathbf{V}, a_3, b_3$). Figure 2 provides a schematic representation of the FCE and VCE models.

[Figure 2 about here.]

Bayesian Inference

We use Markov chain Monte Carlo (MCMC) algorithms to estimate model parameters using Gibbs sampling (Gelfand and Smith 1990). Specific implementation of our Gibbs sampler is discussed in Appendix A. We apply diffuse normal prior distributions for the FCE regression parameters setting $\boldsymbol{\mu}_\beta$ and $\boldsymbol{\mu}_\theta$ equal to zero, σ_β^2 equal to 250, and σ_θ^2 equal to $1e7/k$. The scalar variance hyperparameter for β_i serves as a tuning parameter controlling the degree of smoothness of the penalized spline regression model. We selected a value of 250 based on a gridded search matching as closely as possible penalized spline regression residuals with residuals from a relatively stiff smoothing spline representative of those applied in conventional dendrochronology analyses (i.e. 50 percent frequency response; see Appendix A). We apply non-informative uniform priors for the pure error (σ_{pe}) and inter-annual (τ) standard deviations, but constrain values to an appropriate order of magnitude based on exploratory analysis setting a_1 and a_2 to 0.0001 and b_1 and b_2 to 10.

The same hyperparameter values for $\sigma_\beta^2, a_1, b_1, a_2$ and b_2 are used in the VCE model. The climate coefficient evolution is initialized using a diffuse normal distribution with $\mathbf{m}_0 = \mathbf{0}$ and $\mathbf{C}_0 = \text{Diag}(1e3)$. The temporally-varying climate coefficient estimates are updated using a Kalman filter nested within a Gibbs sampler. We set $\nu = l + 1$ and $\mathbf{V} = \mathbf{I}$ (per Gelman et al. 2014). Finally, we set $a_3 = 0$ and $b_3 = 1$ constraining the η_s 's to an appropriate order of magnitude based on exploratory analysis.

4 Data

Tree Growth Data

Tree growth data was collected in 2010 from 35 forest stands in and around Superior National Forest in northeastern Minnesota (Figure 3; Foster et al. 2014). Stands were selected to represent the predominant forest communities in the broader geographical area based on National Forest Inventory and Analysis data from 2004 to 2008. Specific forest types sampled include aspen/birch, northern hardwood, spruce/fir, mixed pine, and jack pine. Three 400-m² circular plots were established within each stand at least 28 m apart. Increment cores were collected at breast height (1.3 m) from all live trees with a diameter at breast height (DBH) larger than 10 cm. Increment cores were measured using a Velmex measuring stage and crossdated according to standard dendrochronological techniques (Holmes 1983; Yamaguchi 1991). Given issues identifying and measuring recent growth increments, 2007 is the most-recent year for which growth data exist for all trees sampled.

[Figure 3 about here.]

The DBH and species of sample trees were recorded and tree locations were mapped (relative to plot center). Tree age was estimated by defining the pith as the recruitment year and counting the number of growth rings from recruitment to present. Data exist for 2,291 trees representing 15 unique species located across 105 forest plots (Table 1). Sampled forest stands are assumed to have established following a land-clearing disturbance event (e.g. timber harvest or fire). Stand age was estimated by setting the year of establishment equal to the 25th percentile of the tree recruitment year distribution for each stand. The start of the study period is set to 1897 to be consistent with the earliest available climate data, although the growth records for a subset of trees date back before 1897 (study period = 1897 to 2007). As is the case with nearly all dendrochronology datasets, the number of trees and stands observed each year increases with time reflecting trees that established between the start and end of the study period.

[Table 1 about here.]

Forest Tent Caterpillar

The forest tent caterpillar (*Malacosoma disstria*) is an important defoliating insect in northeastern Minnesota. There have been several forest tent caterpillar (FTC) outbreaks in the region during the study period. Most notably, FTC outbreaks resulted in significant defoliation of susceptible trees during the following periods: 1951-1959; 1964-1972; 1989-1995; 2000-2006 (Reinikainen et al. 2012). FTC defoliation in 2001 was particularly severe with greater than 7.5 million acres of susceptible hardwood forests suffering defoliation (Albers et al. 2014). Study species that are known FTC hosts include: *Acer saccharum* (sugar maple), *Betula papyrifera* (paper birch), *Populus grandidentata* (big-tooth aspen), *P. tremuloides* (quaking aspen), and *Quercus rubra* (red oak).

Climate Data

Mean monthly temperature and precipitation estimates were obtained for the study period at a 4-km resolution from PRISM (PRISM Climate Group 2013). Climate data were assigned to individual stands by intersecting plot centroids with the PRISM grid, averaging climate observations across the three stand plots if they fell within different grid cells (occurs for 3 out of 35 stands). A number of studies have shown that temperature and precipitation are poorly correlated with plant distribution and growth in comparison to water balance metrics that translate raw climate observations into variables with direct physiological relevance to plant function (Stephenson 1998; Dyer 2004; Lutz et al. 2010). We derived monthly values of potential evapotranspiration (PET), actual evapotranspiration (AET), climatic water deficit (DEF: PET - AET), and mean snow pack using a modified Thornthwaite-type water balance model (Lutz et al. 2010; see Appendix B for details). We calculated seasonal aggregations for each variable where relevant as detailed in Table 2 for a total of 28 climate variables.

[Table 2 about here.]

Bayesian Variable Selection: We applied the Bayesian Lasso to select a reduced set of climate variables with the greatest effect on annual tree growth (Park and Casella 2008). While not a formal model-based variable selection technique, the Bayesian Lasso shrinks the coefficient values for unimportant variables to zero in a regression model. We chose to apply the Bayesian Lasso given its ability to accommodate collinear variables since many of our climate variables were correlated. Additional details on the Bayesian Lasso and its implementation are provided in Appendix A. The 28 climate variables were pared down to a final set of five climate variables: Fall DEF (FAL-DEF), Spring DEF (SPR-DEF), Summer DEF (SUM-DEF), Summer DEF in the year previous to the year of growth (SUM-DEF-LAG), and mean annual snow pack (SNOW). All model results are restricted to this final set of climate variables.

5 Results

FCE Model

There is strong evidence that annual stand-level tree growth is sensitive to variability in climatic water deficit and snow pack. Specifically, the four deficit variables (FAL-DEF, SPR-DEF, SUM-DEF, SUM-DEF-LAG), where larger values indicate greater water deficit, negatively affected mean annual growth at the stand level, while SNOW positively affected mean annual growth at the stand level (Figure 4). The SNOW variable captures spring recharge of the soil water given the parametrization of the water balance model (see Appendix B). Thus, there is evidence that tree growth in northeastern Minnesota over the last 100 years responds strongly to water availability. The climate coefficient estimates under the FCE model represent the average effects of the five climate variables over the study period.

[Figure 4 about here.]

VCE Model

Estimates of annual effects for each of the five climate variables are obtained applying the VCE model. The evolution of each variable over time is presented in Figure 5. The results of the VCE model differ from the FCE model. The temporally-varying effects of each climate variable are centered around zero. There is no evidence that mean annual growth at the stand level is sensitive to fall deficit in any year during the study period (Figure 5a). For all other deficit variables and snow pack, there is evidence that mean annual growth at the stand level is sensitive to each variable in a subset of years (SPR-DEF: 1952; SUM-DEF: 1910, 1961; SUM-DEF-LAG: 1945, 1988-1994; SNOW: 1952-1953, 1967-1969, 1986) with no evidence of sensitivity to climate variables in the majority of years (Figure 5b-e).

[Figure 5 about here.]

Increased sensitivity to summer deficit occurs in years with large observed summer deficit values (Figure 6b). In particular, a large drought event occurred in northern Minnesota in 1910 leading to increased fire activity (Clark 1989). Increased sensitivity to all other deficit variables and snow pack does not correspond with climate extremes—that is, years exhibiting large

deviations from the mean climate variable value for the study period (Figure 6a,c-d). Rather, there is evidence of correspondence between increased sensitivity to spring deficit (1952), lagged summer deficit (1988-1994), and snow pack (1952-1953, 1967-1969) and the occurrence of regional FTC outbreaks. Further investigation suggests that during periods of correspondence between regional FTC outbreaks and increased sensitivity to climate, the species of trees driving large, stand-level growth decreases relative to mean annual growth in all study stands (indicative of FTC defoliation) are FTC hosts (Figure 7).

[Figure 6 about here.]

[Figure 7 about here.]

Forecasting Tree Growth

The goal of the current analysis is inference regarding the effects of climate variability on annual tree growth. However, both the FCE and VCE models can be used to forecast future tree growth as a function of climate. We applied both models to the northeastern Minnesota dataset holding out the last five years of the study period (2003-2007). The predictive performance of the FCE and VCE models is roughly equivalent based on continuous ranked probability score, root mean square prediction error, coverage rate, and credible interval width (Table 3; see Appendix A for details on scoring statistics). Individual tree growth forecasts using the VCE model are presented for a selection of trees in Figure 8. Results are comparable applying the FCE model.

[Table 3 about here.]

[Figure 8 about here.]

6 Discussion

Fixed Climate Effects

The Bayesian Lasso allows us to identify the most important climate variables from a large set with no *a priori* decisions about which variables to consider and without adjustments for collinearity (Hooten and Hobbs 2015). The value of such a tool in analyses of the effects of climate on ecological processes is great and has not been previously employed in climate ecology studies. We find that water balance variables (climatic water deficit and snow pack) have the greatest impact on inter-annual tree growth in northeastern Minnesota. Water availability is particularly important in the study region where soils are largely formed from glacial till with poor water retention and summers can be quite dry. It is surprising that in a region as cold as northeastern Minnesota, where temperature might be considered to have the greatest effect on inter-annual tree growth, the Bayesian Lasso identifies water balance variables capturing the interaction between temperature and precipitation as more important than temperature metrics alone. The results of the FCE model indicate that tree growth is sensitive to all five water balance variables selected by the Bayesian Lasso over the study period with climatic water deficit exhibiting negative growth effects regardless of season, and snow pack (a measure of spring soil water recharge) exhibiting positive growth effects.

Variable Climate Effects

The results of the VCE model support our hypothesis that tree growth response to climate variability is not fixed with respect to time. The VCE model results suggest that tree growth is sensitive to the most important climate variables in punctuated intervals of one to several years. There is no evidence that tree growth is sensitive to any of the five climate variables during the study period outside of these intervals. A potential cause for short intervals of increased tree growth sensitivity to climate is large annual deviations from long-term mean climate conditions (i.e. climate extremes). The frequency of climate extremes are forecast to increase with global climate change. The VCE model allows for comparison of tree growth response to climate under extreme conditions relative to average climatic conditions. In northeastern Minnesota, tree growth exhibits greater sensitivity to summer deficit during drought years (1910, 1961). For all other climate variables, years in which there is evidence of increased growth sensitivity do not correspond to extreme climate years. This implies that increased sensitivity to climate results from complex interactions involving multiple climate variables and forest ecosystem state. The observed correspondence between FTC outbreaks and increased climate sensitivity in the study region supports this hypothesis. The FCE model does not allow for any inference regarding changes in tree growth sensitivity to climate over time. Instead, there are strong average effects of each climate variable over the entire study period.

Some of the decrease in tree growth sensitivity to climate under the VCE model versus FCE model may be due to the reduced sample size used to estimate climate coefficients. At most 35 stand effects are available to inform annual climate coefficient sets under the VCE model (one effect for each stand), whereas stand effects are pooled across years in the FCE model such that climate coefficients are estimated using 2,764 stand effects. The process equation for temporally-varying climate coefficients (Equation 5) drives the evolution of climate effects when there are insufficient data (stand effects) to constrain coefficient estimates. If annual sample sizes were increased leading to higher tree growth sensitivity to climate in all years under the VCE model, we expect the periods highlighted in Figure 5 to still exhibit increased sensitivity to climate relative to other years in the study period thereby maintaining the correspondence with FTC outbreaks demonstrated in Figure 6.

There is a well studied interaction between FTC defoliation and tree sensitivity to limited water availability with drought events frequently preceding FTC outbreaks (Mattson and Haack 1987; Roth et al. 1997). In particular, recent decline of aspen in northeastern Minnesota has been linked to a combination of reduced water availability and FTC defoliation with drought events facilitating and prolonging FTC outbreaks (Worrall et al. 2013). The observed correspondence between FTC defoliation and increased sensitivity to reduced water availability suggests that FTC defoliation is positively related to water stress and can be explained by several proposed mechanisms: higher concentrations of nitrogen and simple sugars in the leaves of drought-stressed trees facilitate FTC survival and growth; increased leaf temperatures due to reduced stomatal conductance under drought conditions provide more hospitable and attractive habitat for the FTC; and, drought stress lessens the effectiveness of trees' natural defenses (Mattson and Haack 1987). While the interaction between FTC defoliation and drought is established, the VCE model is novel in that it allows for analysis of changes in tree growth response to limited water availability during periods of insect disturbance. The connection between the FTC and increased sensitivity to water balance variables in the study region is

qualitative as we lack data on if and when specific stands were impacted by the FTC. To the extent that such data exist, changes in the growth-climate relationship can be modeled explicitly as a function of FTC presence-absence.

The correspondence between FTC outbreaks and increased sensitivity to water balance observed in northeastern Minnesota is just one example of the additional inference regarding changes in the growth-climate relationship over time made possible by the VCE modeling approach. The VCE model can also be applied to study the temporal interaction between climate and non-FTC disturbances (e.g. other forest pests, fire, management) or dynamic forest processes including succession and stand development. Such applications require data on factors affecting the health and state of the forest ecosystem (e.g. pest presence-absence, stem density, species assemblage) in addition to tree growth records. The VCE model can be extended to explicitly predict changes in the growth-climate relationship as a function of these factors given that relevant data exist. We discuss several specific extensions of the VCE model aimed at improving understanding of the interactive effects of climate and ecosystem state on forest productivity in the *Model Extensions* section. Importantly, traditional dendrochronology and forest ecology models that estimate the average effect of climate on tree growth over time—as in the FCE model—are not able to identify temporal changes in the growth-climate relationship and, hence, do not offer any of the additional inferences described here.

Forest Management Implications

Much of modern applied forest ecology focuses on understanding the effects of climate on forest processes in order to develop management strategies to maintain the composition and structure of existing forest types under climate change. The results of the VCE model imply that it is not enough to understand the relationship between individual tree growth and climate without considering the forest ecosystem as a whole and how shifts in the forest system affect the growth-climate relationship. To be effective, forest management strategies must integrate the effects of climate on forest productivity with the state of the forest system as determined by ecological factors such as stand composition, stem density, disturbance regime, and management history. Strategies need to account for the dynamic nature of forests, modifying applied management over time as the state of the forest ecosystem changes. Of particular importance is the finding that tree growth is not sensitive to climate in the majority of years with increased sensitivity during periods of disturbance. This creates a potentially challenging scenario for forest management in which forest growth is resilient to changing climate until an exogenous factor such as a disturbance event alters the forest ecosystem state leading to sudden changes in forest productivity that may result in significant biomass losses. While perhaps not damaging at a local scale, if large biomass losses were to occur at a regional scale it might affect terrestrial carbon pools with direct ramifications for the global carbon cycle.

Ecological Application

The FCE and VCE model frameworks are not limited to tree growth ring applications. They can be applied in any analysis where interest is in understanding the effects of climate on an ecological process. The FCE model provides a statistically valid approach to integrate coarse-resolution climate data with individual-level observations common in ecological analyses.

The VCE model allows the effects of climate on an ecological process to be analyzed in relation to ecosystem state. We suspect that a wide variety of ecosystems and ecological processes exhibit the same varied effects of climate over time due to shifts in ecosystem state that we observe in the current study. The only requirement for application of the VCE model is appropriate data: repeated measurements through time with sufficient sample size at each time point to inform coefficient estimates.

We note if interest is in forecasting an ecological process as a function of climate, the FCE and VCE models perform equally well. The FCE model is simpler and easier to fit than the VCE model and is preferred if interest is in prediction alone. The VCE model is preferred if interest is in understanding the effect of climate on an ecological process as it offers additional insight regarding changes in the climate-process relationship without sacrificing predictive performance.

Model Extensions

There are several possible extensions to the VCE model aimed at improving understanding of the interactive effects of ecosystem dynamics and climate on forest productivity and health. Analyzing the effects of climate on the entire forest ecosystem requires the use of censused tree growth ring records collected in closed canopy forests where growth is affected by inter-tree competition and microsite variation in addition to climate. An important question is whether these closed canopy records should be detrended to remove the effects of tree size and age. Such records frequently do not exhibit the expected negative exponential decrease in annual growth increment over time. Instead, closed canopy records show the effects of past forest dynamics with distinct periods of growth suppression and release (from competition). In smoothing over such periods through the use of flexible spline-based models, we may remove important ecosystem dynamics signals. An alternative approach is to replace the detrending component of the VCE model with a forest growth process model that explicitly represents forest stand dynamics (e.g. SORTIE). This would partition the effects of forest dynamics and climate on tree growth and allow for closer examination of climate effects in relation to ecosystem state. A second extension of the VCE model with the same goal in mind is to replace the random walk model for the evolution of climate effects over time with a model that incorporates ecological factors known to affect forest ecosystem state including pest presence-absence, stand density, and percent canopy cover. In northeastern Minnesota, for example, change in climate effects over time could be modeled as a function of FTC presence-absence (we lack the necessary data to apply this approach in the current analysis). Models would initially be phenomenological, but as understanding of the factors driving changes in the growth-climate relationship improved, could be updated with mechanistic process models.

Finally, we note our current approach of mapping climate observations to forest stands by intersecting stand centroids with coarse climate grid cells is ad hoc; although, it is an improvement over current studies that apply gridded climate data at the scale of individual trees. An alternative is to develop a formal spatial model to map coarse climate observations to forest stands. Such a model would account for the spatial dependence structure that exists in climate data and explicitly estimate uncertainty introduced by applying climate data at a new spatial scale.

7 Conclusions

We have demonstrated the relationship between climate and tree growth is not constant with respect to time, but varies in relation to forest ecosystem state. In northeastern Minnesota, forests exhibit heightened sensitivity to water availability during FTC outbreak years. Changes in tree growth sensitivity to climate are not observable fitting conventional models that estimate the average effect of climate on growth over time. While the interaction between drought stress and FTC outbreaks has been previously established, a model for tree growth as a function of climate capable of identifying changes in the growth-climate relationship due to this interaction is novel.

The results of this study underscore the importance of considering the entire forest ecosystem when studying the effects of climate on forest productivity. To this end, the VCE model provides a powerful framework for understanding the interaction between ecosystem dynamics and climate on forest growth and health. The VCE model has broad application in ecology offering valuable insight to any study where the goal is understanding the effects of climate on ecological processes.

8 Acknowledgments

The authors thank Christopher Wikle, Giovanni Petris, and Neil Pederson for their helpful comments and feedback during the drafting of this paper. This work was supported by National Science Foundation Grants DMS-1513481, EF-1137309, EF-1241874 and EF-1253225 and the Northeast Climate Science Center.

9 Literature Cited

- Albers, J., Albers, M., and Cervenka, V. (2014). Forest tent caterpillar fact sheet. *Minnesota Department of Natural Resources*.
- Babst, F., Alexander, M. R., Szejner, P., Bouriaud, O., Klesse, S., Roden, J., Ciais, P., Poulter, B., Frank, D., Moore, D. J. P., and Trouet, V. (2014). A tree-ring perspective on the terrestrial carbon cycle. *Oecologia*, 176(2):307–322.
- Bonan, G. B. (2008). Forests and climate change: forcings, feedbacks, and the climate benefits of forests. *Science*, 320(5882):1444–1449.
- Calder, C., Lavine, M., Müller, P., and Clark, J. S. (2003). Incorporating multiple sources of stochasticity into dynamic population models. *Ecology*, 84(6):1395–1402.
- Carrer, M. (2011). Individualistic and time-varying tree-ring growth to climate sensitivity. *PLoS One*, 6(7):e22813.
- Clark, J. S. (1989). Effects of long-term water balances on fire regime, north-western Minnesota. *Journal of Ecology*, 77(4):989–1004.
- Clark, J. S., Bell, D. M., Kwit, M., Stine, A., Vierra, B., and Zhu, K. (2012). Individual-scale inference to anticipate climate-change vulnerability of biodiversity. *Philosophical Transactions of the Royal Society B: Biological Sciences*, 367(1586):236–246.

- Clark, J. S. and Bjørnstad, O. N. (2004). Population time series: process variability, observation errors, missing values, lags, and hidden states. *Ecology*, 85(11):3140–3150.
- Clark, J. S., Wolosin, M., Dietze, M., Ibáñez, I., LaDeau, S., Welsh, M., and Kloeppel, B. (2007). Tree growth inference and prediction from diameter censuses and ring widths. *Ecological Applications*, 17(7):1942–1953.
- Cook, E. R. (1987). The decomposition of tree-ring series for environmental studies. *Tree-Ring Bulletin*, 47:37–59.
- Cook, E. R. and Kairiukstis, L. A., editors (1990). *Methods of Dendrochronology: Applications in the Environmental Sciences*. Kluwer Academic Publications, Hingham, MA.
- Cook, E. R. and Peters, K. (1981). The smoothing spline: a new approach to standardizing forest interior tree-ring width series for dendroclimatic studies. *Tree-Ring Bulletin*, 41:45–53.
- Cressie, N. and Wikle, C. K. (2011). *Statistics for Spatio-Temporal Data*. John Wiley & Sons, Hoboken, NJ.
- Dyer, J. M. (2004). A water budget approach to predicting tree species growth and abundance, utilizing paleoclimatology sources. *Climate Research*, 28(1):1–10.
- Dymond, S. F., D’Amato, A. W., Kolka, R. K., Bolstad, P. V., Sebestyen, S. D., and Bradford, J. B. (2015). Growth-climate relationships across topographic gradients in the northern great lakes. *Ecohydrology*.
- Fajardo, A. and McIntire, E. J. B. (2012). Reversal of multicentury tree growth improvements and loss of synchrony at mountain tree lines point to changes in key drivers. *Journal of Ecology*, 100(3):782–794.
- Foster, J. R., D’Amato, A. W., and Bradford, J. B. (2014). Looking for age-related growth decline in natural forests: Unexpected biomass patterns from tree rings and simulated mortality. *Oecologia*, 175(1):363–374.
- Fritts, H. C. (1976). *Tree Rings and Climate*. Academic Press Inc., London.
- Galván, J. D., Camarero, J. J., and Gutiérrez, E. (2014). Seeing the trees for the forest: Drivers of individual growth responses to climate in *Pinus uncinata* mountain forests. *Journal of Ecology*, 102(5):1244–1257.
- Gelfand, A. and Smith, A. F. M. (1990). Sampling-based approaches to calculating marginal densities. *Journal Of The American Statistical Association*, 85(410):398–409.
- Gelman, A. (2006). Prior distributions for variance parameters in hierarchical models (Comment on Article by Browne and Draper). *Bayesian Analysis*, 1(3):515–534.
- Gelman, A., Carlin, J. B., Stern, H. S., and Rubin, D. B. (2014). *Bayesian Data Analysis*. Taylor & Francis, 3 edition.

- Holmes (1983). Computer-assisted quality control in tree-ring dating and measurement. *Tree-Ring Bulletin*, 43(1):69.
- Hooten, M. B. and Hobbs, N. T. (2015). A guide to Bayesian model selection for ecologists. *Ecological Monographs*, 85(1):3–28.
- Hooten, M. B., Wikle, C. K., Dorazio, R. M., and Royle, J. A. (2007). Hierarchical spatiotemporal matrix models for characterizing invasions. *Biometrics*, 63(2):558–567.
- Leites, L., Robinson, A., Rehfeldt, G., Marshall, J., and Crookston, N. (2012). Height-growth response to changes in climate differ among populations of interior Douglas-fir: a novel analysis of provenance-test data. *Ecological Applications*, 22(1):154–165.
- Littell, J. S., Peterson, D. L., and Tjoelker, M. (2008). Douglas-fir growth in mountain ecosystems: Water limits tree growth from stand to region. *Ecological Monographs*, 78(3):349–368.
- Lutz, J. A., van Wagendonk, J. W., and Franklin, J. F. (2010). Climatic water deficit, tree species ranges, and climate change in Yosemite National Park. *Journal of Biogeography*, 37(5):936–950.
- Mattson, W. J. and Haack, R. a. (1987). The Role of Drought in Insects of Plant-eating Outbreaks Drought ' s physiological effects on plants can predict its influence on insect populations. *BioScience*, 37(2):110–118.
- Park, T. and Casella, G. (2008). The Bayesian Lasso. *Journal of the American Statistical Association*, 103(482):681–686.
- Parslow, J., Cressie, N., Campbell, E. P., Jones, E., and Murray, L. (2013). Bayesian learning and predictability in a stochastic nonlinear dynamical model. *Ecological Applications*, 23(4):679–698.
- PRISM Climate Group (2013). Oregon State University, <http://prism.oregonstate.edu>, created 15 Aug 2013.
- Reinikainen, M., D'Amato, A. W., and Fraver, S. (2012). Repeated insect outbreaks promote multi-cohort aspen mixedwood forests in northern Minnesota, USA. *Forest Ecology and Management*, 266:148–159.
- Roth, S., McDonald, E. P., and Lindroth, R. L. (1997). Atmospheric CO₂ and soil water availability: consequences for tree-insect interactions. *Canadian Journal of Forest Research*, 27(8):1281–1290.
- Schliep, E. M., Dong, T. Q., Gelfand, A. E., and Li, F. (2014). Modeling individual tree growth by fusing diameter tape and increment core data. *Environmetrics*, 25(8):610–620.
- Schofield, M. R., Barker, R. J., Gelman, A., Cook, E. R., and Briffa, K. R. (2015). A model-based approach to climate reconstruction using tree-ring data. *Journal of the American Statistical Association*, (just-accepted):1–30.

- Stephenson, N. L. (1998). Actual evapotranspiration and deficit: biologically meaningful correlates of vegetation distribution across spatial scales. *Journal of Biogeography*, 25:855–870.
- Van Deusen, P. C. (1989). A model-based approach to tree ring analysis. *Biometrics*, 45(3):763–779.
- Wikle, C. K. (2003). Hierarchical Bayesian models for predicting the spread of ecological processes. *Ecology*, 84(6):1382–1394.
- Wood, S. (2006). *Generalized Additive Models: An Introduction with R*. CRC press, Boca Raton, FL.
- Worrall, J. J., Rehfeldt, G. E., Hamann, A., Hogg, E. H., Marchetti, S. B., Michaelian, M., and Gray, L. K. (2013). Recent declines of *Populus tremuloides* in North America linked to climate. *Forest Ecology and Management*, 299:35–51.
- Yamaguchi, D. K. (1991). A simple method for cross-dating increment cores from living trees. *Canadian Journal of Forest Research*, 21(3):414–416.
- Zhu, K., Woodall, C. W., Ghosh, S., Gelfand, A. E., and Clark, J. S. (2014). Dual impacts of climate change: forest migration and turnover through life history. *Global Change Biology*, 20(1):251–264.

Table 1: Summary of species sampled.

Species	Species Code	Number of Trees	Number of Plots	First Year Observed	% Relative Basal Area
<i>Abies balsamea</i>	ABBA	365	59	1897	4.4
<i>Acer rubrum</i>	ACRU	87	30	1899	2.6
<i>Acer saccharum</i>	ACSA	175	16	1899	8.9
<i>Betula papyrifera</i>	BEPA	273	50	1897	15.1
<i>Fraxinus nigra</i>	FRNI	132	9	1897	6.8
<i>Larix laricina</i>	LALA	10	6	1903	0.2
<i>Picea glauca</i>	PIGL	96	30	1929	4.2
<i>Picea mariana</i>	PIMA	400	36	1897	14.5
<i>Pinus banksiana</i>	PIBA	383	23	1919	16.2
<i>Pinus resinosa</i>	PIRE	33	9	1903	3.6
<i>Pinus strobus</i>	PIST	56	15	1898	6.8
<i>Populus grandidentata</i>	POGR	23	4	1927	1.9
<i>Populus tremuloides</i>	POTR	93	25	1925	5.3
<i>Quercus rubra</i>	QURU	118	11	1919	3.8
<i>Thuja occidentalis</i>	THOC	47	12	1897	5.6

Notes: Number of plots is the number of plots in which each species is found. First year observed is the first year in the study period a growth record exists for a tree of the corresponding species (some trees have records that date back prior to 1897). Percent relative basal area is based on tree diameters in 2010.

Table 2: Summary of seasonal aggregations of climate variables. Bullets indicate that a seasonal aggregation is calculated for a given variable.

Variable	Fall (Sep - Nov) _{t-1}	Winter (Dec - Feb) _t	Spring (Mar - May) _t	Summer (Jun - Aug) _t	Summer Lag (Jun - Aug) _{t-1}
Mean Tmin	•	•	•	•	•
Mean Tmean	•	•	•	•	•
Mean Tmax	•	•	•	•	•
Total AET	•		•	•	•
Total PET	•		•	•	•
Total DEF	•		•	•	•
Mean SNOW		•			

Notes: Tmin, Tmean, Tmax indicate minimum, mean, and maximum temperature, AET and PET indicate actual and potential evapotranspiration, DEF indicates climatic water deficit (PET - AET), SNOW indicates snow pack. Subscripts, t = year of growth, $t - 1$ = year preceding growth.

Table 3: Out-of-sample scoring statistics for FCE and VCE models applied to tree growth data with final five years (2003-2007) of data held out to demonstrate forecasting.

Model	CRPS	RMSPE	Coverage Rate	Mean 95% CI Width
FCE	0.78	1.65	0.90	4.80
VCE	0.78	1.64	0.91	4.85

Notes: CRPS = continuous ranked probability score (lower values preferred); RMSPE = root mean square prediction error (lower values preferred); CI = credible interval (lower values preferred).

List of Figures

1	Graphical depiction of climate coefficient evolution and VCE model dependencies with arrows indicating direct dependence.	23
2	Schematic of FCE and VCE tree growth models. <i>Note:</i> Fixed and variable climate effects sub-models are applied separately; $0:T$ subscript indicates all time points from 0 to T	24
3	Location of 105 forest plots (35 stands, 3 plots per stand) in relation to Superior National Forest in northeastern Minnesota, USA.	25
4	Standardized coefficient values for FCE model. <i>Note:</i> Points represent posterior median coefficient estimates; black lines indicate 95 percent credible interval bounds; a dashed grey line at a coefficient value of zero is provided for reference.	26
5	Evolution of standardized coefficient values over the study period for VCE model. <i>Note:</i> Thick black lines represent posterior median coefficient estimates; grey shaded regions indicate 95 percent credible interval (CI) bounds; a dashed grey line at a coefficient value of zero is provided for reference; years in which the lower bound of the CI is greater than zero are highlighted in green; and years in which the upper bound of the CI is less than zero are highlighted in red.	27
6	Evolution of standardized coefficient values for the VCE model in relation to climate variables. Upper plots show mean climate values across stands (thick black line) with corresponding 95 percent confidence intervals (grey shading). Lower plots show time-varying coefficient values (thick black line = posterior median; grey shading = 95 percent credible interval). Years in which the lower bound of the CI is greater than zero are highlighted in green and years in which the upper bound of the CI is less than zero are highlighted in red. Black polygons indicate years in which FTC outbreaks occurred in the region: (1) 1951-1959; (2) 1964-1972; (3) 1989-1995; (4) 2000-2006.	28
7	Violin plots of partial residuals (observed log annual growth increment minus spline-based estimate) for FTC host and non-host individuals located in stands in the 10th percentile for growth in years a) 1952-1953; b) 1967-1969; c) 1988-1994. Stands in the lowest 10th percentile for growth are considered likely to have been affected by FTC. <i>Note:</i> Black shading indicates FTC host trees; grey shading indicates non-FTC host trees.	29
8	Predicted annual log growth increments for a sample of eight trees. <i>Note:</i> Thick grey line = posterior mean predicted growth; dashed lines = 95 percent posterior prediction interval bounds; points = observed log growth increment where grey shading indicates data was used to fit the model and open points indicate data was held out. All tree growth data was held out from 2003 to 2007 to demonstrate forecasting. Subplot labels indicate tree I.D. number and species (see Table 1 for species codes).	30

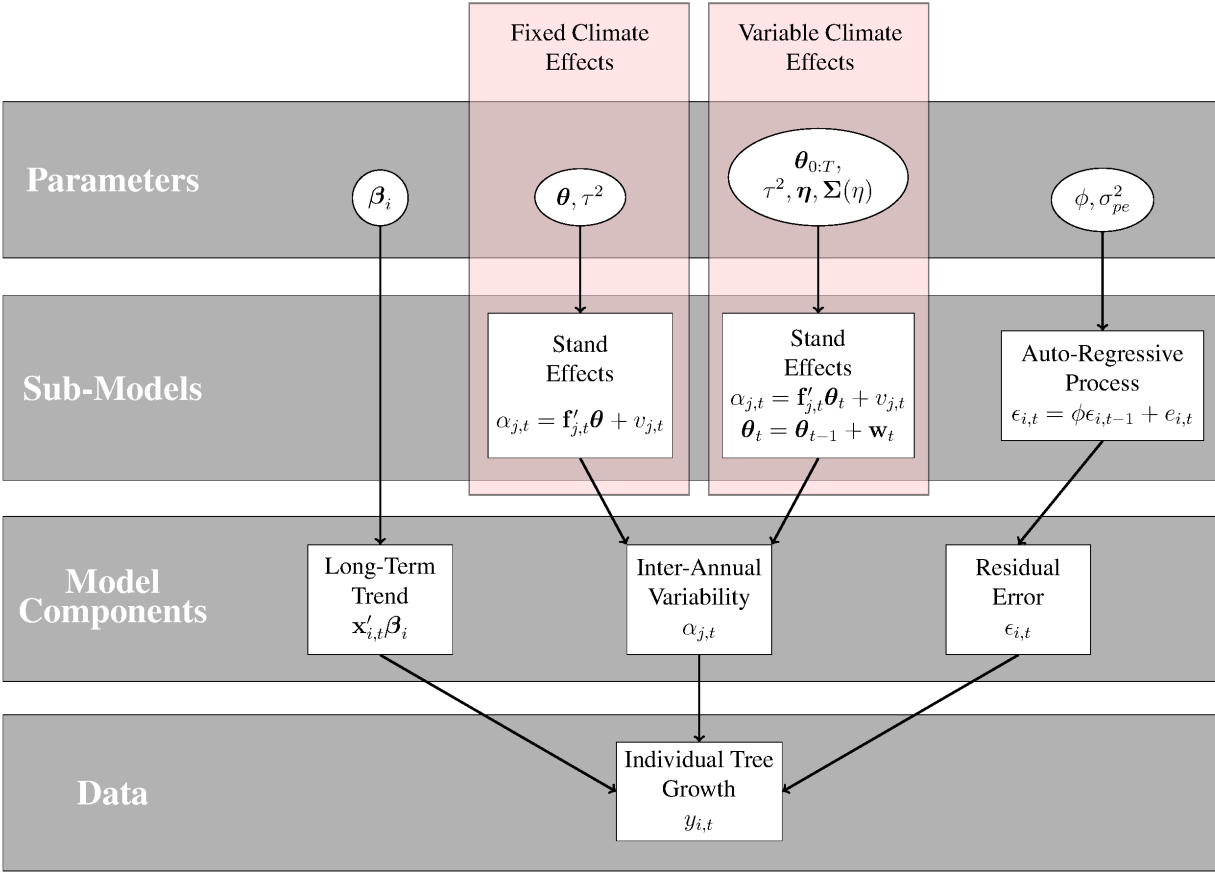


Figure 2

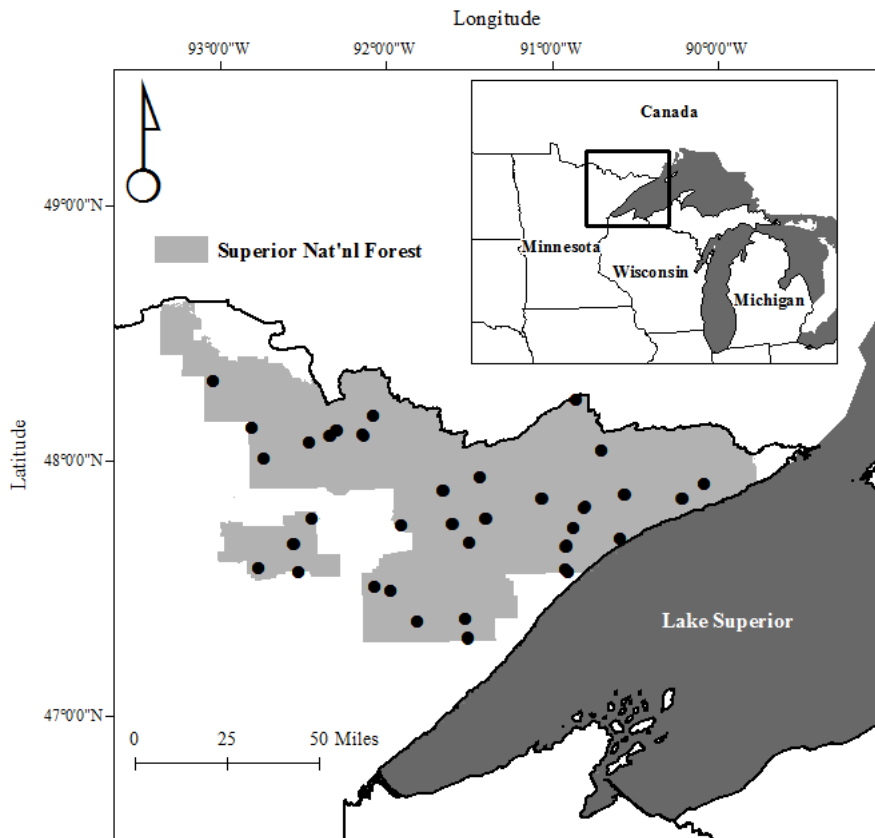


Figure 3

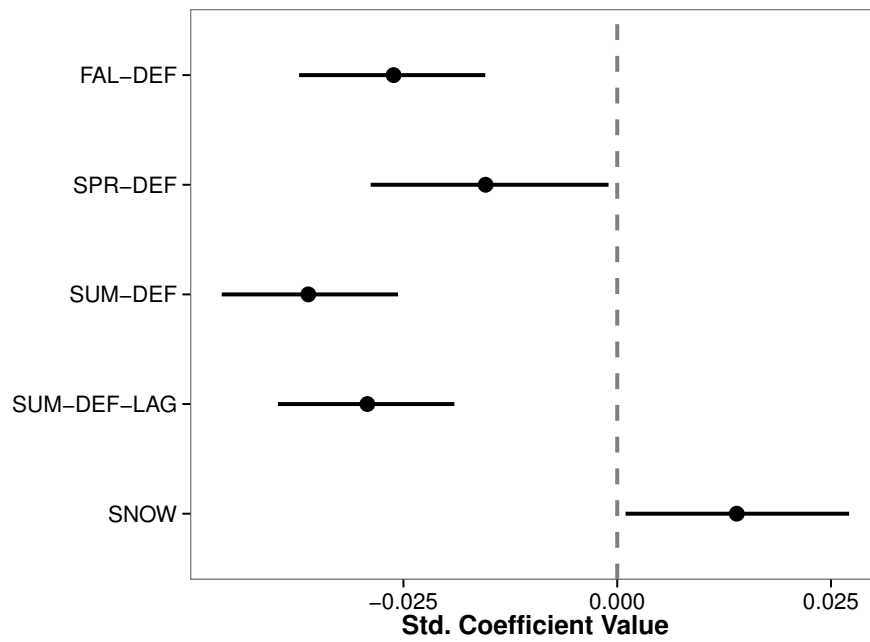


Figure 4

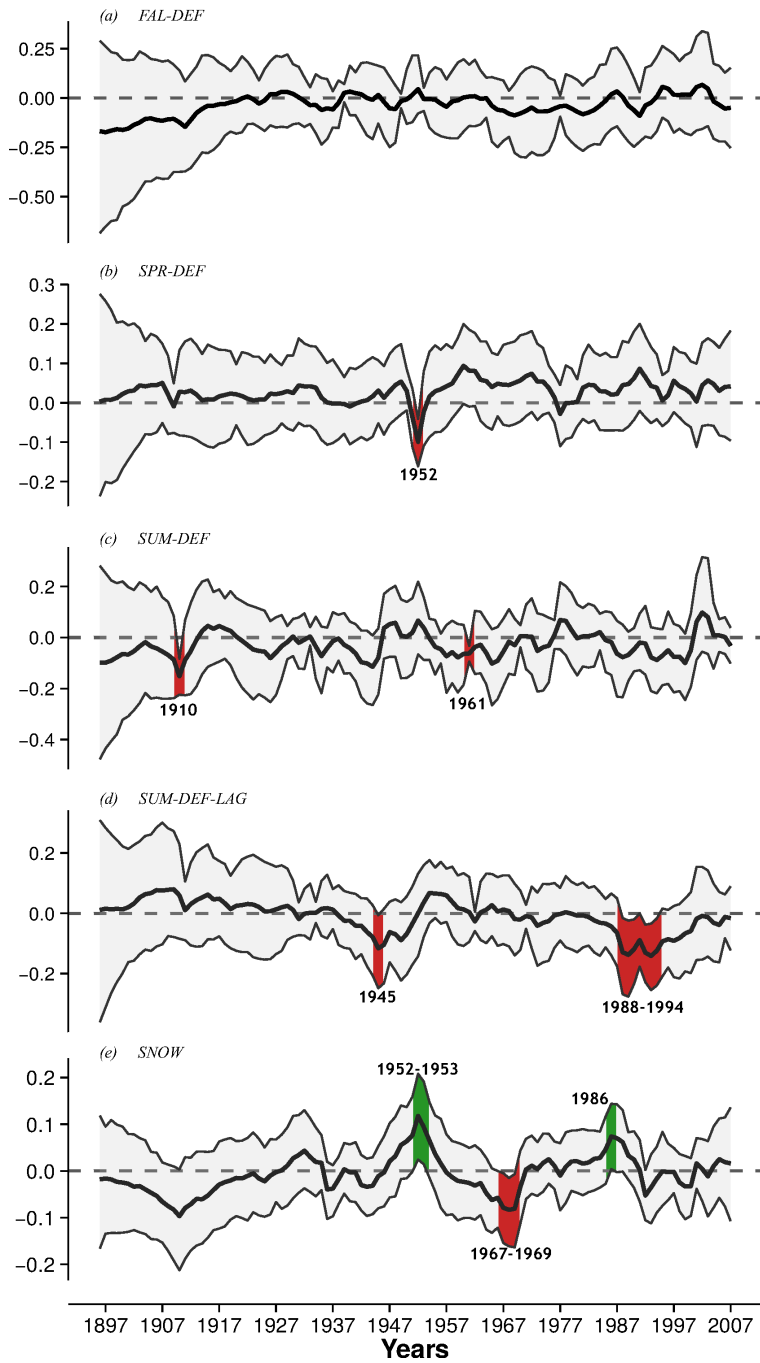


Figure 5

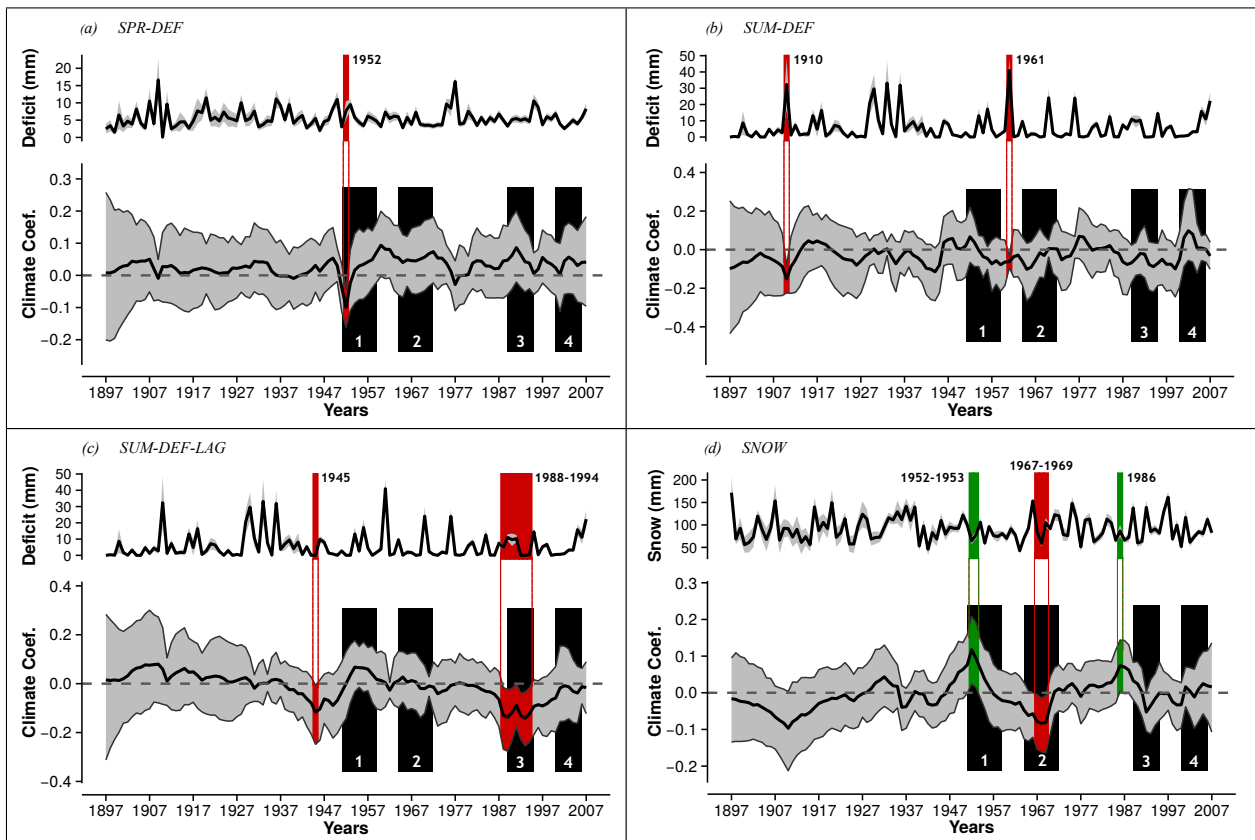


Figure 6

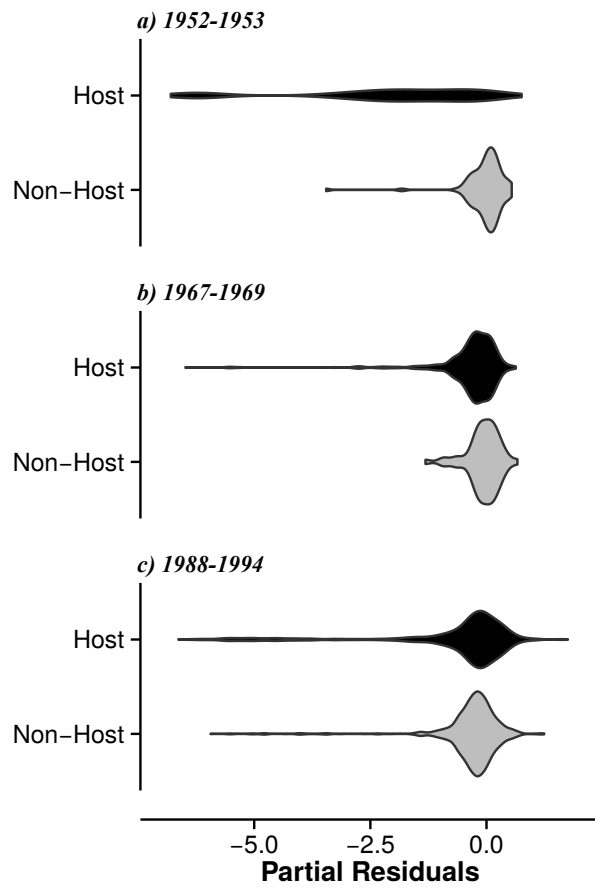


Figure 7

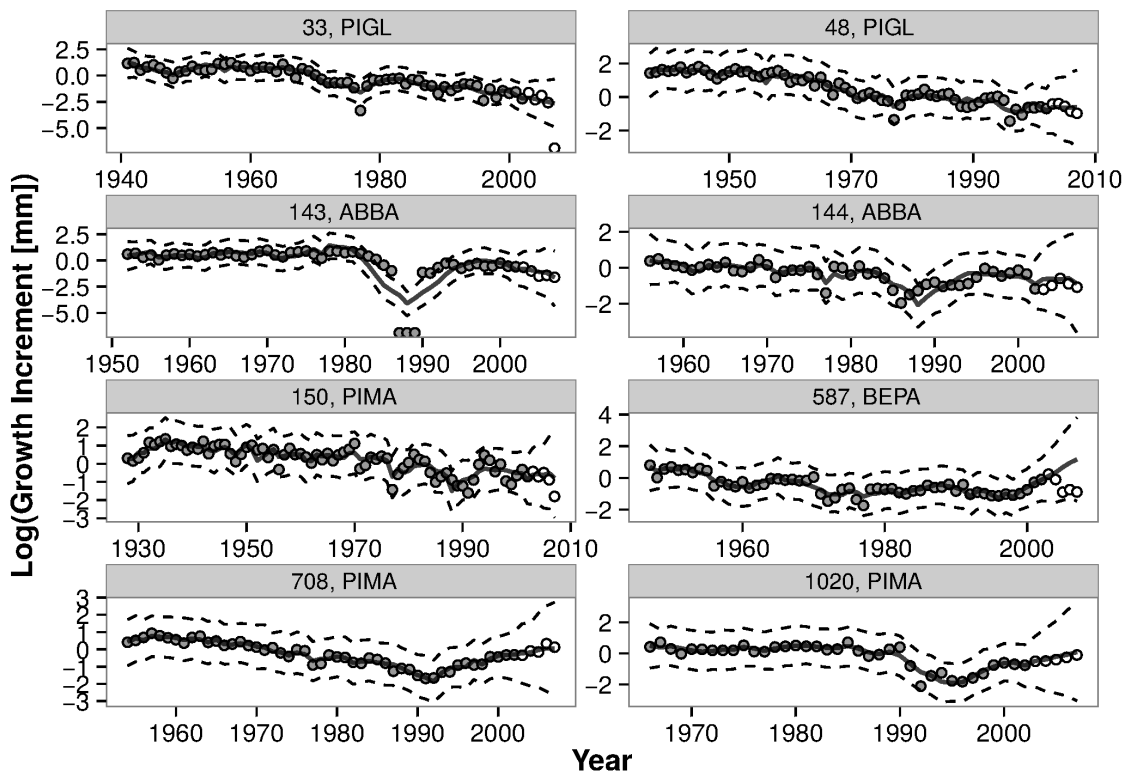


Figure 8